Title

Load transfer between pile groups and laterally spreading ground during earthquakes.

Authors

Brandenberg, SJ

Boulanger, RW

Kutter, BL

et al.

Publication Date

2023-12-11

Peer reviewed

13th World Conference on Earthquake Engineering
Vancouver, B.C., Canada
August 1-6, 2004
Paper No. 1516

LOAD TRANSFER BETWEEN PILE GROUPS AND LATERALLY SPREADING GROUND DURING EARTHQUAKES

Scott J. BRANDENBERG[1], Ross W. BOULANGER[2], Bruce L. KUTTER[2], Dan W. WILSON[3], Dongdong CHANG[4]

SUMMARY

The lateral load transfer between pile groups and laterally spreading ground during earthquakes is evaluated based on results of dynamic model tests on a 9-m-radius centrifuge. The pile groups consisted of six piles, with prototype diameters of either 0.73 m or 1.17 m, connected together by a pile cap embedded in a soil profile consisting of a gently sloping nonliquefied crust over liquefiable loose sand over dense sand. Realistic earthquake motions with peak base accelerations ranging from 0.13 g to 1.00 g were applied to each of the models. The observed patterns of deformation throughout the centrifuge models are described in detail to illustrate several important features of behavior. A typical dynamic response is presented, showing components of the soil-pile and soil-pile cap interaction forces that were measured directly or obtained by data processing. Procedures for estimating the total horizontal loads on an embedded pile cap (i.e., passive loads plus friction along the base and sides) are discussed. Relative displacements between the free-field soil and pile cap required to mobilize the peak horizontal loads from the crust are shown to be much larger than expected for static loading conditions. The reasons for this softer-than-expected lateral load transfer behavior are discussed, and a simple idealization is used to illustrate the mechanism by which liquefaction of the underlying sand affected the load transfer behavior of the overlying crust. A simple relation for describing the observed lateral load transfer behavior between the pile caps and nonliquefied crusts is subsequently presented.

INTRODUCTION

Loads imposed on pile foundations by laterally spreading ground during earthquakes have been a major cause of past damages and are consequently a major concern in design practice. The cost can be very large to construct a new pile foundation, or retrofit an existing pile foundation, to resist the expected loads from laterally spreading ground, especially when a relatively strong surface layer is spreading over an underlying liquefied layer. However, the actual loading mechanisms between laterally spreading ground and pile foundations are only approximately understood.

[1] Graduate student, University of California, Davis. Email: sjbrandenberg@ucdavis.edu
[2] Professor, University of California, Davis
[3] Facility Manager, Center for Geotechnical Modeling, University of California, Davis
[4] Graduate student, University of California, Davis.

Recent model tests, including centrifuge tests (Wilson et al. [1], Abdoun et al. [2]), full-scale shaking table tests (Tokimatsu et al. [3]) and load tests in blast-induced liquefied soil (Ashford and Rollins [4]) have helped characterize several important aspects of soil-pile interaction in liquefied sand. However, only a limited number of physical model studies of pile groups in liquefied and laterally spreading ground have been performed.

This paper addresses the lateral load transfer behavior between pile groups and laterally spreading soil during earthquake shaking based on a series of dynamic centrifuge model tests. First, the centrifuge model testing program is described, and then the observed patterns of deformation throughout the centrifuge models are used to illustrate several important features of behavior. A typical dynamic response showing various components of the soil-pile and soil-pile cap interaction forces is presented and discussed. The contributions of passive pressures, side friction, and base friction to the total horizontal load exerted on the embedded pile cap are evaluated. Then the lateral load transfer behavior is presented in terms of the relative displacements between the free-field soil and pile cap required to mobilize various fractions of the peak horizontal loads from the crust. This load transfer behavior is shown to be much softer than expected for static loading conditions, after which the reasons for this observed behavior are discussed in detail. In particular, a simple idealization is used to illustrate the mechanism by which liquefaction of the underlying sand affects the load transfer behavior of the overlying crust. A simple relation for describing the observed lateral load transfer behavior between the pile caps and nonliquefied crusts is subsequently presented.

CENTRIFUGE MODELS

The centrifuge tests were performed on the 9-m radius centrifuge at the University of California at Davis. All tests were performed in a flexible shear beam container with centrifugal accelerations ranging from 36 to 57 g. Results are presented in prototype units.

A schematic cross-section of one centrifuge model is shown in Figure 1. The soil profile consisted of a nonliquefied crust overlying loose sand ($D_r \approx$ 21-35%) overlying dense sand ($D_r \approx$ 69-83%). The crust layer sloped gently toward a river channel carved in the crust at one end of the model. The nonliquefiable crust consisted of reconstituted San Francisco Bay mud (liquid limit ≈ 88, plasticity index ≈ 48) that was mechanically consolidated with a large hydraulic press, and subsequently carved to the desired slope. The sand layers beneath the crust consisted of uniformly graded Nevada Sand (C_u = 1.5, D_{50} = 0.15 mm). A thin layer of coarse Monterey sand was placed on the surface of the Bay mud for some of the models.

The six-pile group for the model in Figure 1 consisted of 1.17-m diameter piles with a large pile cap embedded in the nonliquefied crust. The pile cap provided fixed-head restraint at the connection with the piles. Some tests contained a single-degree-of-freedom superstructure fixed to the top of the pile cap, and superstructures with various natural periods were tested.

Each test was shaken with a number of simulated earthquakes conducted in series with sufficient time between shakes to allow dissipation of excess pore pressures. The simulated earthquakes were scaled versions of the acceleration recordings either from Port Island (83-m depth, north-south direction) during the Kobe earthquake, or from the University of California, Santa Cruz (UCSC/Lick Lab, Channel 1) during the Loma Prieta earthquake. These earthquake motions were chosen because they contain different frequency content and shaking characteristics. Generally, the shake sequence applied to the models was a small event ($a_{max,base}$ = 0.13g to 0.17g) followed by a medium event ($a_{max,base}$ = 0.30g to 0.45g) followed by one or more large events ($a_{max,base}$ = 0.67g to 1.00g).

Details for these centrifuge experiments are summarized in a series of data reports available from the web site for the Center for Geotechnical Modeling (http://cgm.engr.ucdavis.edu) (e.g. Brandenberg et al. [5]).

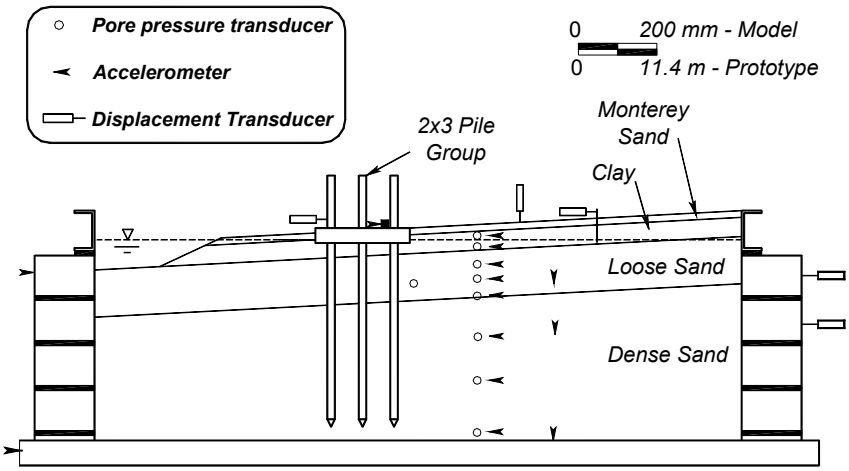

Figure 1. Schematic layout of a centrifuge model with a pile group in laterally spreading ground.

These data reports include detailed explanations of model construction, data acquisition procedures, data organizational structure, post-earthquake model dissection measurements, and all instrument recordings.

OBSERVED DEFORMATION PATTERNS IN CENTRIFUGE MODELS

Deformations within the centrifuge models were measured during shaking and then further documented during dissection of the models after testing. The post-testing photographs illustrate a number of important features of behavior, as described below.

An overhead view of a centrifuge model after testing (looking down onto the model surface) is shown in Figure 2. The soil is sloping downhill from the right side toward the left side of the photograph. The cracks in the crust were caused by large displacements as the crust spread downslope on top of the underlying liquefiable layer.

A second overhead view of the same model is shown in Figure 3 after the surface layer of sand had been vacuumed off the top of the underlying clay. Several grids of light-colored bentonite clay had been placed on the clay surface to measure the displacement patterns caused by shaking. The grid locations before shaking have been drawn on the figure in dashed white lines and the grid locations after shaking have been outlined in solid white lines with arrows connecting the before and after lines. The deformation patterns of the lines show that the concentrated large strains immediately upslope from the pile cap decrease gradually with distance upslope from the cap. The influence of the cap on the strains in the clay is still evident in the curved bentonite grid line that was farthest upslope from the clay, on the far right of Figure 3.

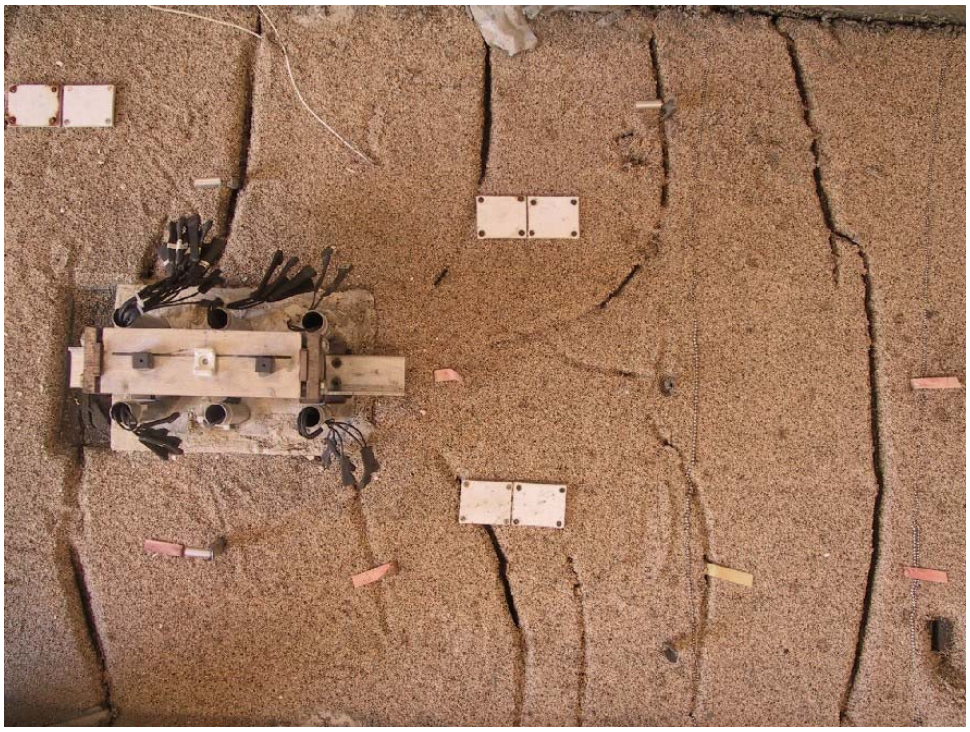

Figure 2. Photograph looking down onto model DDC02 after it has been removed from the centrifuge arm and the various instrumentation racks have been removed (ground slopes downhill to the left)

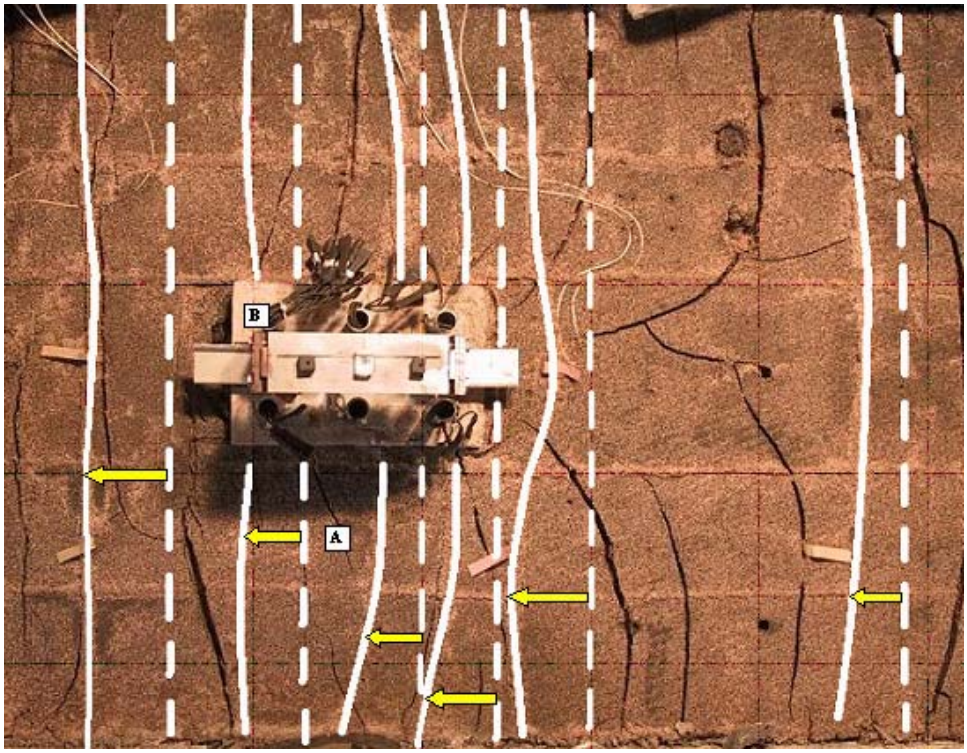

Figure 3. Photograph looking down onto model DDC02 after the surface layer of sand has been removed (dashed white lines show the "before" shaking positions of the marker lines, while the solid white lines highlight their "after" shaking positions).

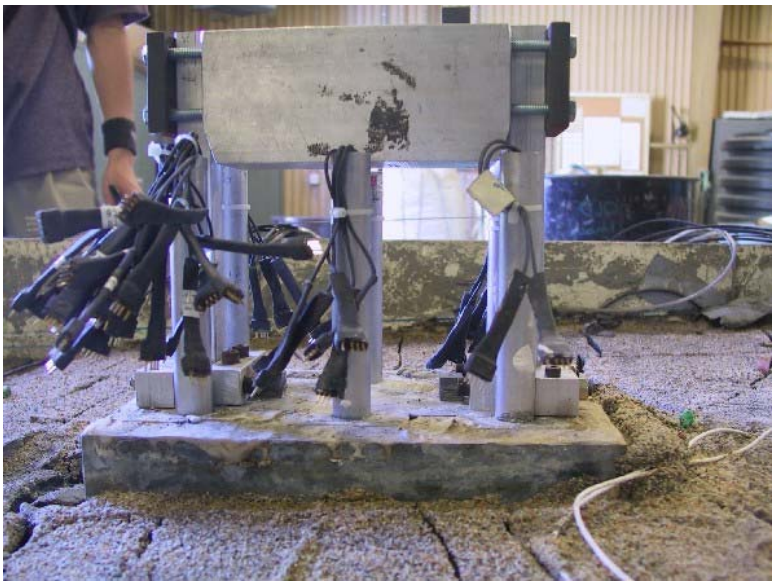

Figure 4. Side view of the pile cap, still embedded in the clay layer, after the surface layer of sand has been removed (Note the passive bulge on the uphill/right side).

The photo in Figure 3 also shows that the displacements of the crust near the sides of the pile cap were smaller than the displacements near the walls of the container. The smaller displacements near the pile cap are attributed to the restraining loads imposed on the crust by the pile group (including the side and base frictional forces). The friction between the crust and container walls (an undesirable boundary effect) was minimized in this test by cutting a thin slot (i.e., the width of a knife blade) through the crust along its contact with the container wall, and then injecting bentonite slurry into the slot prior to testing of the model. The bentonite slurry would then consolidate when the centrifuge model was spun to its final centrifugal acceleration, but would still represent a much lower frictional boundary than would otherwise have existed between the overconsolidated crust and the container walls. For centrifuge models that did not have a bentonite-filled slot, the average lateral spreading displacements were somewhat smaller but the pattern of displacements was very similar. Thus the surface markers for the various tests showed that the pile groups strongly affected deformation patterns in the clay crust to large distances away, a fact that later will be important for understanding the observed lateral load transfer behavior.

A close-up side view of the pile cap is shown in Figure 4, again after the surface layer of sand had been removed. The soil surface is the top of the clay layer, a gap has formed behind the downstream side of the cap (left side of the photo) and a passive bulge has formed on the upstream side (right side of the photo).

The progressive excavation of the various centrifuge models after shaking exposed several important features of the subsurface deformation profile. Figure 5 shows a side view of a pile cap after the soil to its side has been excavated, exposing the passive bulge that formed against the upslope side of the pile cap. The soils were then excavated from beneath the pile cap to expose the supporting piles. Figure 6 shows the side view of the exposed piles, from which a couple of points are noted. First, the clay layer opened gaps on the downhill sides of the piles (left sides of piles in the photo) as the clay spread downslope, and the underlying liquefied sand boiled up into the gaps. Second, the sides of the piles within the underlying sand layer are coated with a thin layer of clay that was dragged downward during driving of the piles (prior to spinning of the centrifuge). This downward smearing of the clay affects the axial shaft friction on the piles within the sand layers, as has previously been noted in the literature. Figure 7 shows a side view of the contact between the overlying clay and the liquefiable sand layer, as exposed during

Figure 5. Side view of a pile cap after the adjacent soil has been excavated (Note the passive bulge on the uphill [right] side).

Figure 6. Side view of the piles beneath the cap after the adjacent soil has been excavated (Note the sand that has boiled into the gaps behind the piles, as the clay spread from right to left).

excavation at a location upslope from the pile cap. The deformed shape of vertical markers (softened spaghetti noodles or paper strips), such as shown in this photo, repeatedly showed the formation of a localized zone of sliding along the interface. This localization is attributed to void redistribution (or water film formation) that is driven by the accumulation of upwardly seeping pore water as it is impeded by the overlying low permeability clay layer (e.g., see Malvick et al. [6]).

Figure 7. Side view of the contact between the liquefying loose sand layer and the overlying clay layer, with a vertical marker showing the discontinuity in deformation at the interface.

TYPICAL TIME HISTORIES OF RESPONSE

The dynamic responses of the centrifuge models were well defined by over 100 instruments in each model, including accelerometers, pore pressure transducers, displacement transducers, and strain gauge bridges on the piles, as schematically illustrated in Figure 1. In addition, time histories of various load components were obtained by processing the raw instrumentation recordings. In particular, a free-body diagram for a pile cap is shown in Figure 8. Of the forces acting on a pile cap, the pile cap inertia, $k_h \cdot W$ and shear forces, $2 \cdot V_s$, $2 \cdot V_c$ and $2 \cdot Vn$, were obtained directly by instrumentation recordings. Additionally, the loading on the pile segments above the strain gauges was estimated by back-calculation of p-time histories obtained by numerically double differentiating the moment distributions with depth along the piles according to the equation

$$p(z) = \frac{d^2}{dz^2} M(z).$$

From horizontal dynamic equilibrium of this free-body, the sum of the passive force on the upslope face of the cap, horizontal friction between the sides of the cap and the crust, and horizontal friction between the base of the cap and the crust (Passive + F_1 + F_4) could be calculated. The individual contributions of these three quantities could not be obtained independently based on the measured data, but analytical predictions of the three quantities can provide insight into the mechanisms of loading imposed on the cap. The passive force was estimated using Coulomb earth pressure theory. The friction force between the clay and the sides and base of the pile cap ($F_{1,clay}$) was estimated using $F_{1,clay} = \alpha\, c_u\, A_{sides,c}$, where α is the adhesion coefficient and $A_{sides,c}$ is the contact area between the clay and the pile cap. The friction force between the Monterey sand and the sides of the pile cap ($F_{1,sand}$) was estimated using $F_{1,sand} = \frac{1}{2}\, \gamma\, K_o H_1 \tan(\delta)\, A_{sides,s}$ where K_o, the coefficient of earth pressure at rest, was taken as $1\text{-}\sin(\phi')$, $A_{sides,s}$ is the contact area between the Monterey sand and the pile cap. The friction force on the base of the pile cap was calculated as $F_4 = \alpha\, c_u\, A_{base}$, where A_{base} is the area of the base of the pile cap minus the area of the piles. Details of the calculations of the load components and results for different tests were presented by Boulanger et al. [7].

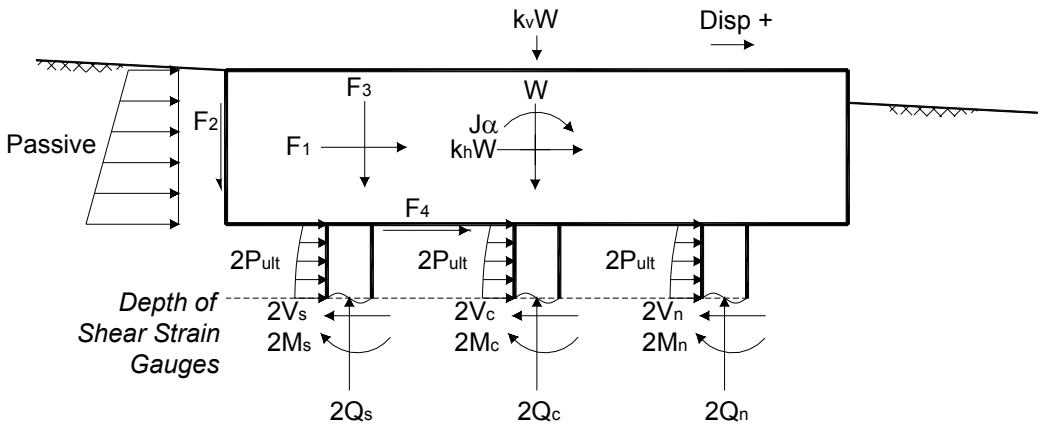

Figure 8. Free-body diagram for a pile cap from the centrifuge models.

The back-calculations of the components of crust loads on the pile caps are straightforward in principle, but there are several important details that can affect the reliability of the calculations. Loads on the pile segments between the bottom of the cap and the shear strain gauge bridges, back-calculated by double-differentiation of moment distributions along the pile, were subtracted from the shear loads measured at the strain gauge bridges to obtain the crust loads on the pile cap. The double-differentiation can be prone to errors immediately adjacent to the pile cap connection and near soil layer interfaces where the distribution of lateral load changes sharply. However, the load distribution near the midpoint between the base of the cap and the liquefiable sand layer, which was used in the calculations, is believed to be accurate. Additionally, the calculations did not account for interaction between the friction on the base of the cap and the loads imposed by the pile segments on the clay. Nevertheless, the measured load was under-predicted if base friction was neglected, even with $\alpha = 1$ at the interface between the sides of the cap and the clay. The values of α that gave good agreement between measured lateral loads and calculated lateral loads (assuming base friction develops) for different centrifuge tests are summarized in Boulanger et al. [7].

The results of the above analyses indicate that the passive force exerted on the upslope face of the pile cap ranged from only 48% to 63% of the crust load on the pile cap, with side and base friction accounting for the remaining fraction. While neglecting the friction forces may be conservative in design when the pile cap is being relied upon to resist lateral loading imposed by a superstructure, neglecting the friction forces in cases when a crust is spreading laterally and imposing loads on the pile cap would be unconservative. Furthermore, base friction is often ignored by designers based on the assumption that a gap will form as the clay settles away from the pile cap. However, the gap may close as the crust comes in contact with the bottom of the cap as lateral spreading causes the clay to wedge between the pile cap and the underlying soil layers. Therefore, a designer must be certain that the gap will remain during lateral spreading if base friction is to be neglected for design.

Time histories are shown in Figure 9 for various components of the dynamic response from model SJB03, where sign conventions are positive in the directions drawn in Figure 8. This particular set of time histories is for a large Kobe earthquake event ($a_{max,base}$ = 0.67 g), which was preceded by a large Santa Cruz event ($a_{max,base}$ = 0.67 g), a medium Santa Cruz event ($a_{max,base}$ = 0.35 g) and a small Santa Cruz event ($a_{max,base}$ = 0.13 g).

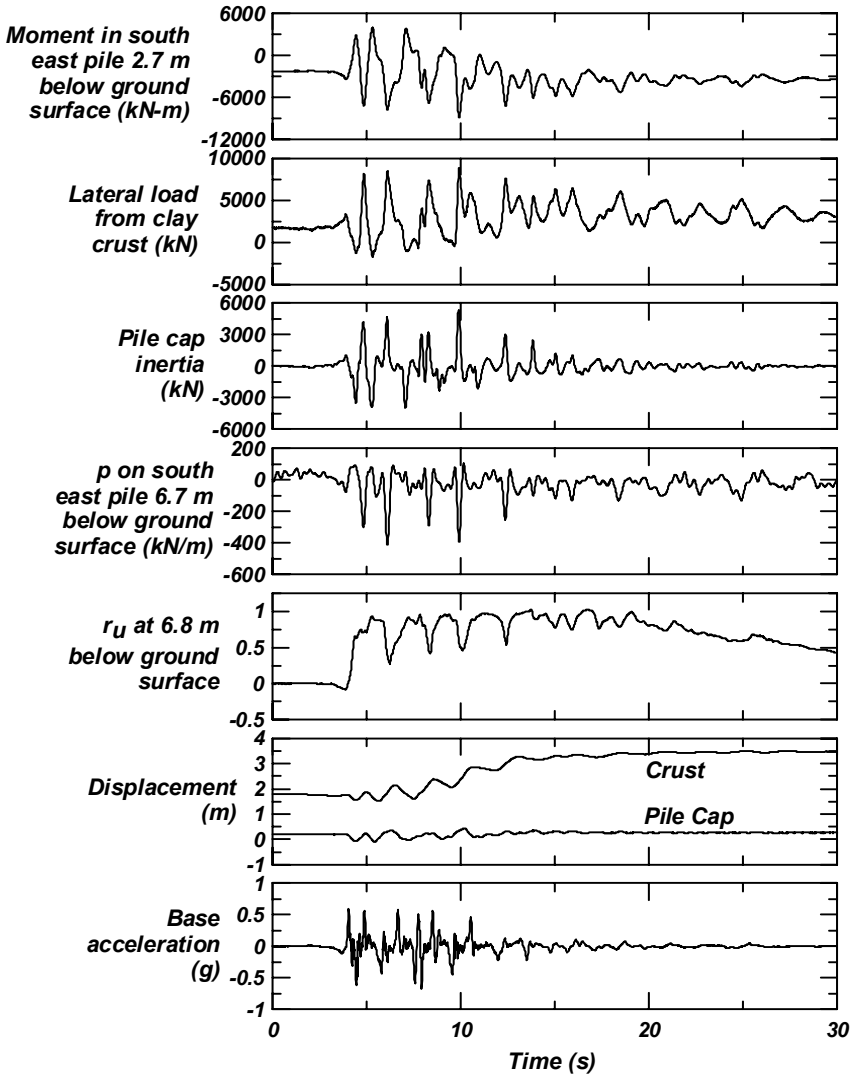

Figure 9. Time histories from model SJB03 during a large Kobe earthquake with a peak base acceleration of 0.67 g.

These time histories illustrate a number of important features of dynamic response.

- r_u near the center of the liquefiable sand layer (at 6.8-m depth) reached a value near unity at about time = 5 s. Later in shaking, r_u transiently dropped to smaller values near 0.5, which were accompanied by transient increases in effective stress, and hence in strength and stiffness of the sand.
- The critical cycle that produced the peak moment (-8838 kN·m) and peak lateral load from the clay crust (8826 kN) occurred at about time = 10 s, when r_u near the center of the liquefiable sand was at a local minimum of 0.5 in spite of having been near 1 previously, and returning to near 1 later during strong shaking.
- The middle of the liquefiable sand layer (6.7 m below the ground surface) provided a large upslope resisting load (-400 kN/m) to the piles during the critical loading cycle.
- The peak lateral load from the crust occurred at about 10 seconds, but the peak relative displacement between the pile cap and the free-field crust occurred near the end of shaking.

Certain aspects of the loading mechanics observed during the centrifuge tests are different from assumptions that are commonly made in design practice. For example, the liquefiable sand provided a large upslope resisting load during the critical loading cycles, which is contrary to the common assumption that liquefied sand imposes a small downslope loading on the piles in the direction of soil displacement. As an example, the Japan Road Association [8] suggests using $p = 0.3 \cdot \sigma_v \cdot b$, where p is the lateral load exerted by the liquefied sand. Near the center of the liquefiable sand in the centrifuge tests, $0.3 \cdot \sigma_v \cdot b$ = 41 kN/m, which is an order of magnitude different from and opposite in sign from the measured p-value during the critical loading cycle (p = -400 kN/m). In addition, the peak lateral load from the clay crust occurred during the time of strong shaking, even though the greatest relative cap-soil displacement occurred toward the end of shaking. This observation is important to the development of guidelines on how to combine kinematic and inertial load components in simplified design procedures.

OBSERVED LOAD-TRANSFER RELATION BETWEEN PILE CAP AND CLAY CRUST

The total lateral load from the crust is plotted versus the relative displacement at virgin loading peaks (i.e. crust load peaks that exceed the maximum past crust load) in Figure 10. Each virgin peak load was normalized by the greatest overall peak load measured for that specific model test. The relative displacement was taken as the soil displacement to the side of the pile cap (at point A in Fig. 3) minus the pile cap displacement (at point B in Fig. 3). This relative displacement was then normalized by pile cap height. The resulting data show that the overall peak lateral loads were mobilized at relative displacements of 40% to over 100% of the pile cap height, which is much larger than commonly expected.

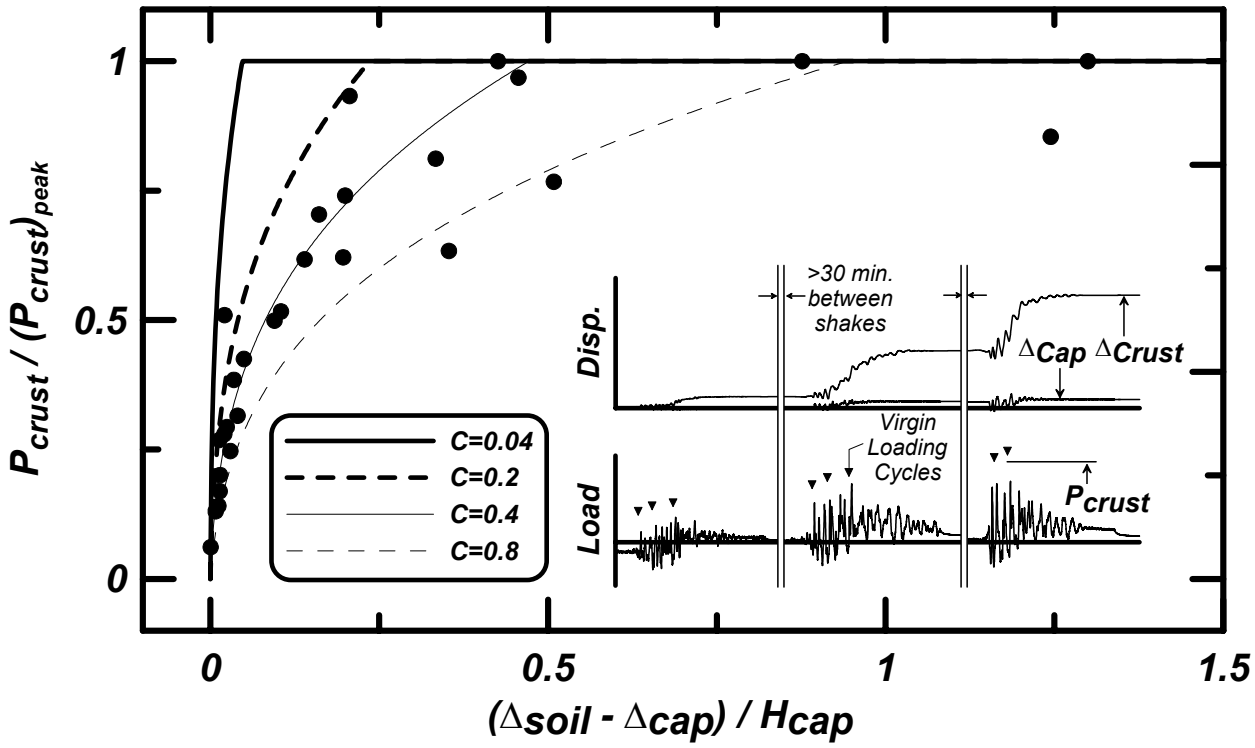

Figure 10. Normalized lateral load from the surface crust versus the relative cap-soil displacement.

The load transfer relation shown in Figure 10 is much softer than expected based on common experiences with static loading tests. Static loading of retaining walls and pile caps have shown that full passive resistance is mobilized when the wall displacement is more than about 1% to 5% of the wall height, depending on soil type and density. For example, Rollins and Sparks [9] performed static load tests on a pile group in granular soil and reported that the peak load was mobilized at a pile cap displacement of about 2.5% to 6% of the pile cap height. Duncan and Mokwa [10] and Mokwa and Duncan [11] describe load tests on bulkheads and pile groups embedded in sandy silt/sandy clay and in gravel/sand backfills and showed that passive loads were mobilized at displacements of about 1% to 4% of the pile cap height. In design practice for lateral spreading loads, it is commonly assumed that the load transfer relation is similar to those observed from static loading tests.

DISCUSSION OF THE LATERAL LOAD TRANSFER MECHANISM

The softer-than-expected relation between lateral loads and relative cap-soil displacement, as observed from the centrifuge tests (Figure 10) may be influenced by several factors. For example, cyclic degradation of the clay stress-strain response would cause the lateral load transfer behavior to be softer than for static lateral loading. However, the differences between the static load tests and the centrifuge tests are too large to be explained by cyclic degradation alone.

The softer lateral load transfer behavior during lateral spreading as opposed to static loading is primarily attributed to the effects of liquefaction beneath the surface crust. In particular, liquefaction of the underlying soils has a strong effect on the distribution of stresses in the nonliquefied crust. For static loading of a pile cap without any liquefaction in the underlying soils, some of the stress imposed on the clay by the pile cap would geometrically spread down into the sand and thus stresses in the clay crust would decrease sharply with distance away from the pile cap. For the case where the underlying sand is liquefied, the stress imposed on the clay by the pile cap would not be able to spread down into the liquefied sand (assuming it has essentially zero stiffness compared to the crust), and thus the lateral stress in the clay crust would decrease more slowly with distance away from the pile cap. Spreading of lateral stress to greater distance back from the pile cap causes larger strains in the clay soil away from the pile cap. The spreading of lateral stress is evident in Figure 3, where the light-colored clay markers show that the pile cap induced strains in the clay at a large distance upslope from the cap. Since relative cap-soil displacement represents an integral of strains between two reference points, the result is a much softer load versus relative displacement response for the crust over liquefied soil than for the crust supported on nonliquefied soil.

A simplistic two-dimensional idealization of the lateral loading mechanism provides a clear illustration of the basic mechanisms involved. Consider the lateral loading of the clay layer over liquefied soil as idealized in Figure 11. The clay layer is H thick, L long, and is elastic-plastic with a yield strain, ε_{hf}, of 5%. The bottom boundary of the clay is frictionless due to liquefaction of the underlying soils. The vertical boundaries of the clay are both frictionless, and the left boundary is fixed against translation.

The peak passive lateral force will be reached when the lateral displacement, Δ_{hf}, is:

$$\Delta_{hf} = \varepsilon_{hf} \cdot L$$

which when normalized by the wall height gives the normalized relative displacement of:

$$\frac{\Delta_{hf}}{H} = \frac{\varepsilon_{hf} \cdot L}{H}$$

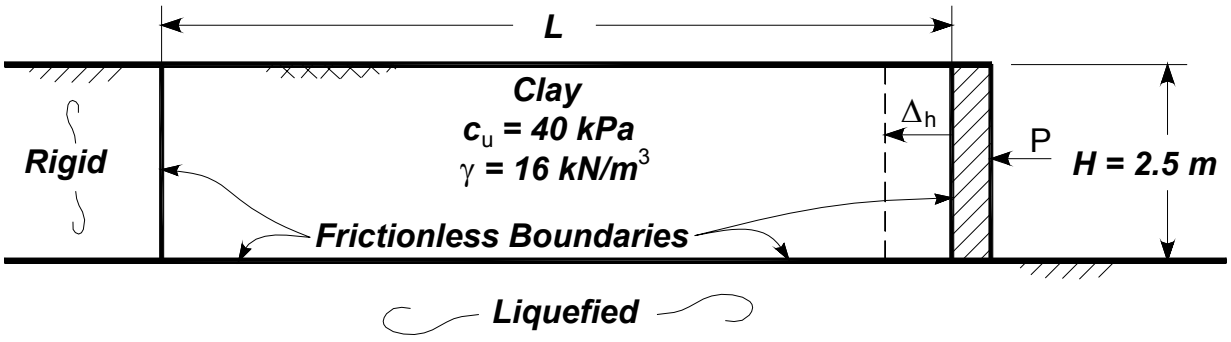

Figure 11. Two-dimensional idealization for illustrating the effect of liquefaction on load transfer between a nonliquefied crust and a pile cap.

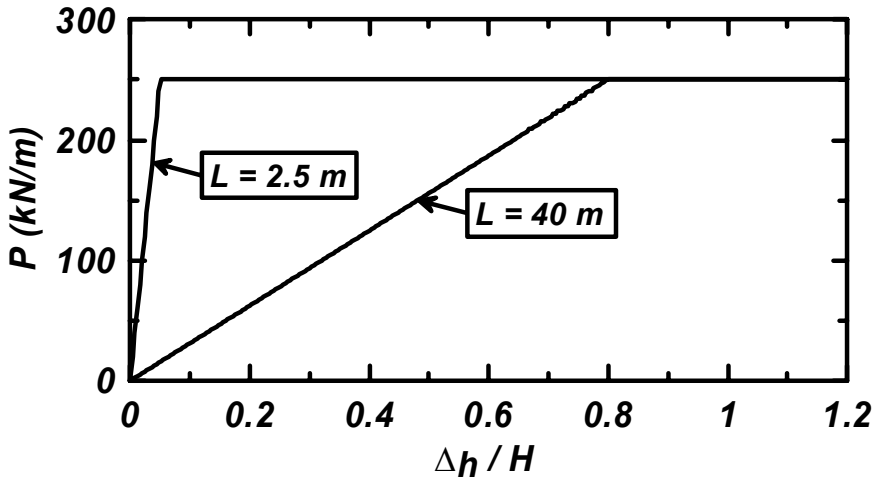

Figure 12. Load transfer relation for idealized 2-D problem with elastic-plastic clay layer over zero-strength layer.

These simple equations are used to produce the plot of normalized lateral load versus normalized displacement in Figure 12. When the clay layer length is equal to the wall height (2.5 m), the peak lateral load is mobilized at a normalized displacement of $\Delta_{hf}/H = 0.05$. In contrast, when the clay layer length is 40 m, the peak lateral load is mobilized at a normalized displacement of $\Delta_{hf}/H = 0.8$.

Terzaghi [12] asserted that the Rankine states of stress (active and passive) are not realistic for natural soil deposits because frictionless boundaries, as shown in Fig. 11, are required to produce a uniform stress distribution throughout the soil deposit. He postulated that elimination of friction between the base of a soil deposit and the underlying soils cannot occur in practice, hence Rankine theory is valid only "in our imagination." Furthermore, Terzaghi noted that these "imaginary" boundary conditions would result in mobilization of Rankine stress states at very large lateral displacements that are proportional to the length of the soil deposit rather than its height. Although Terzaghi's intent was to describe a practical limitation of Rankine earth pressure theory for static loading problems, it is interesting that his assertions turned out to be useful in explaining the soft load-versus-relative-displacement response observed for the case of a

nonliquefied crust spreading laterally over a liquefiable deposit where friction at the bottom of the crust is small due to trapping of upward-seeping pore water beneath the crust.

The two-dimensional plane-strain idealizations shown in Figure 11, and considered by Terzaghi, are much simpler than the truly three-dimensional loading conditions that occur for pile caps of finite width. For three-dimensional loading, stresses would geometrically spread out-of-plane, which would reduce the size of the zone of influence upslope from the pile cap and produce a significantly more complicated distribution of strain. Nonetheless, it is believed that the basic idea of the liquefied layer causing a softening of the lateral load transfer response is a primary factor explaining the observations in Figure 10.

APPROXIMATE RELATION FOR LATERAL LOAD TRANSFER

Two trend lines, one corresponding to "no liquefaction" and one corresponding to "liquefaction" are also shown in Fig. 10. The equation used for the trend lines is

$$\frac{P}{P_u} = \left[\left(\frac{y}{C \cdot H} \right)^{-0.33} + \left(\frac{16 \cdot y}{C \cdot H} \right)^{-1} \right]^{-1} \leq 1$$

where P is the load on the pile cap, P_u is the ultimate load, y is the relative displacement between the free-field crust and the pile cap, H is the height of the pile cap, and C is a constant that controls the stiffness of the curve. The relationship can be visualized as consisting of elastic and plastic components in series. With C = 0.04, the full crust load is mobilized at a relative displacement of about 5% of the pile cap height, which is reasonable for cases without liquefaction. With C = 0.4, the full crust load is mobilized at about 48% of the pile cap height which produces a fit through the middle of the centrifuge test data. Several additional lines have been included in Figure 10 to demonstrate a reasonable range of C-values that nearly envelope the data, and to show the sensitivity of the p-y curve to variations in C.

CONCLUSIONS

Centrifuge models with pile groups embedded in a sloping soil profile with a nonliquefied clay crust overlying liquefiable loose sand over dense sand were shaken with a series of realistic earthquake motions. The nonliquefied crust laterally spread downslope on top of the liquefiable sand, imposing kinematic loads on the pile caps and piles. Photographs and measurements taken after the tests identified several features of the complex loading mechanics, including distributions of displacements of the clay crust.

Observations of the test data indicate that critical loading cycles occurred during transient drops in excess pore pressure in the liquefiable sand, which restrained the piles from moving downslope as the crust slid on top of the liquefiable sand. This loading mechanism contrasts with the common design assumption that liquefied sand imposes a small downslope loading in the direction of soil displacement, which indicates that simplified design procedures are crude approximations that cannot capture many of the more complicated dynamic loading conditions observed in the tests.

Friction between the crust and the sides and base of the pile caps contributed a large portion of the total loads attracted by the pile caps as the crust spread downslope. The laterally spreading crust became wedged between the base of the pile cap and the top of the underlying soil layers, thereby closing any gaps that might have occurred during settlement of the clay prior to shaking. Failure to account for the friction loads along the sides and base of a pile cap would be unconservative for design of pile foundations in laterally spreading soil. Base friction should be excluded only if the designer is confident that a gap will remain beneath the cap during the earthquake.

Large relative displacements between the pile caps and the free-field soil were required to mobilize the peak lateral crust loads against the pile caps. This lateral load transfer behavior was much softer than expected based on analogies to static loading experiences, with the differences attributed primarily to cyclic degradation and the influence of the underlying liquefiable sand. Liquefaction beneath the crust allowed strains in the crust to spread geometrically to a large distance upslope of the pile cap before stresses were sufficient to cause passive failure. The distribution of strains through a larger mass of soil resulted in larger relative displacements since relative displacement is the integral of strain between two reference points. A simple relation for the total lateral crust load (P) versus relative cap-soil displacement (y) was presented that, via its calibration to these centrifuge test data, approximately accounts for the influence of the underlying liquefied soil.

ACKNOWLEDGEMENTS

Funding was provided by Caltrans under contract numbers 59A0162 and 59A0392 and by the Pacific Earthquake Engineering Research (PEER) Center, through the Earthquake Engineering Research Centers Program of the National Science Foundation, under contract 2312001. The contents of this paper do not necessarily represent a policy of either agency or endorsement by the state or federal government. Recent upgrades to the centrifuge have been funded by NSF award CMS-0086566 through the George E. Brown, Jr. Network for Earthquake Engineering Simulation (NEES). Center for Geotechnical Modeling (CGM) staff Tom Kohnke, Tom Coker and Chad Justice provided assistance with centrifuge modeling. Priyanshu Singh oversaw some of the centrifuge tests and performed some data processing.

REFERENCES

1. Wilson, D. W., Boulanger, R. W., and Kutter, B. L. (2000). "Seismic lateral resistance of liquefying sand." *J. of Geotechnical and Geoenvironmental Engrg.,* ASCE, Vol. 126(10), 898-906.
2. Abdoun, T., Dobry, R., O'Rourke, T.D., and Goh, S.H. (2003). "Pile response to lateral spreads: Centrifuge modeling." *J. of Geotechnical and Geoenvironmental Engrg.,* ASCE, 129(10), 869-878.
3. Tokimatsu, K., Suzuki, H., and Suzuki, Y. (2001). "Back-calculated p-y relation of liquefied soils from large shaking table tests." *Fourth International Conference on Recent Advances in Geotechnical Earthquake Engineering and Soil Dynamics*, S. Prakash, ed, Univ. of Missouri – Rolla, paper 6.24.
4. Ashford, S. A., and Rollins, K. M. (2002). *TILT: The Treasure Island Liquefaction Test: Final Report*, Report SSRP-2001/17, Department of Structural Engineering, University of California, San Diego.
5. Brandenberg, S. J., Chang, D., Boulanger, R. W., and Kutter, B. L. (2003). "Behavior of piles in laterally spreading ground during earthquakes – centrifuge data report for SJB03." Report No. UCD/CGMDR-03/03, Center for Geotechnical Modeling, Department of Civil Engineering, University of California, Davis.
6. Malvick, E. J., Kutter, B. L., Boulanger, R. W., and Feigenbaum, H. P. (2004). "Post-shaking failure of sand slope in centrifuge test." Proc., 11th SDEE and 3rd ICEGE, Berkeley, CA.
7. Boulanger, R. W., Kutter, B. L., Brandenberg, S. J., Singh, P., and Chang, D. (2003). *Pile foundations in liquefied and laterally spreading ground during earthquakes: Centrifuge experiments and analyses*. Report UCD/CGM-03/01, Center for Geotechnical Modeling, Univ. of California, Davis, CA, 205 pp.
8. JRA (2002). *Specifications for highway bridges*. Japan Road Association, Preliminary English Version, prepared by Public Works Research Institute (PWRI) and Civil Engineering Research Laboratory (CRL), Japan, November.
9. Rollins, K. M., and Sparks, A. (2002). "Lateral resistance of full-scale pile cap with gravel backfill." *J. of Geotechnical and Geoenvironmental Engrg.,* ASCE, Vol. 128(9), 711-723.
10. Duncan, M.J., and Mokwa, R.L. (2001). "Passive earth pressures: Theories and tests." *J. of Geotechnical and Geoenvironmental Engrg.,* ASCE, Vol. 127(3), 248-257.
11. Mokwa, R.L., and Duncan, M.J. (2001). "Experimental evaluation of lateral-load resistance of pile caps." *J. of Geotechnical and Geoenvironmental Engrg.,* ASCE, Vol. 127(2), 185-192.
12. Terzaghi, K. (1936). "A fundamental fallacy in earth pressure computations." *J. of the Boston Society of Civil Engineers.* April.